Sustained vs. Intratidal Recruitment in the Injured Lung During Airway Pressure Release Ventilation: A Computational Modeling Perspective

Andrea F. Cruz, PhD[*]; *Jacob Herrmann, PhD*[†]; *Harry Ramcharran, MD*[‡]; *Michaela Kollisch-Singule, MD*[‡]; *Merryn H. Tawhai, PhD*[§]; *Jason H.T. Bates, PhD, DSc*[‖]; *Gary F. Nieman, BA*[‡]; *David W. Kaczka, MD, PhD*[*,†,¶]

ABSTRACT

Introduction:

During mechanical ventilation, cyclic recruitment and derecruitment (R/D) of alveoli result in focal points of heterogeneous stress throughout the lung. In the acutely injured lung, the rates at which alveoli can be recruited or derecruited may also be altered, requiring longer times at higher pressure levels to be recruited during inspiration, but shorter times at lower pressure levels to minimize collapse during exhalation. In this study, we used a computational model to simulate the effects of airway pressure release ventilation (APRV) on acinar recruitment, with varying inspiratory pressure levels and durations of exhalation.

Materials and Methods:

The computational model consisted of a ventilator pressure source, a distensible breathing circuit, an endotracheal tube, and a porcine lung consisting of recruited and derecruited zones, as well as a transitional zone capable of intratidal R/D. Lung injury was simulated by modifying each acinus with an inflation-dependent surface tension. APRV was simulated for an inhalation duration (T_{high}) of 4.0 seconds, inspiratory pressures (P_{high}) of 28 and 40 cmH_2O, and exhalation durations (T_{low}) ranging from 0.2 to 1.5 seconds.

Results:

Both sustained acinar recruitment and intratidal R/D within the subtree were consistently higher for P_{high} of 40 cmH_2O vs. 28 cmH_2O, regardless of T_{low}. Increasing T_{low} was associated with decreasing sustained acinar recruitment, but increasing intratidal R/D, within the subtree. Increasing T_{low} was associated with decreasing elastance of both the total respiratory system and transitional subtree of the model.

Conclusions:

Our computational model demonstrates the confounding effects of cyclic R/D, sustained recruitment, and parenchymal strain stiffening on estimates of total lung elastance during APRV. Increasing inspiratory pressures leads to not only more sustained recruitment of unstable acini but also more intratidal R/D. Our model indicates that higher inspiratory pressures should be used in conjunction with shorter exhalation times, to avoid increasing intratidal R/D.

INTRODUCTION

Severe trauma is a major problem in combat-related casualties and can progress into acute respiratory distress syndrome (ARDS), especially for injured military personnel deployed to austere combat environments.[1] Current clinical management of ARDS is largely supportive and typically includes positive pressure mechanical ventilation. However, cyclic recruitment and derecruitment (R/D) of alveoli during mechanical ventilation can result in foci of parenchymal stress, from which inflammation and edema develop and spread.[2] The result of these processes is progressive ventilator–induced lung injury (VILI), which itself can be fatal.

The development and progression of VILI can be significantly mitigated through the avoidance of cyclic R/D, as has been demonstrated both theoretically and experimentally.[2–5] Achieving this goal clinically, however, is complicated by the fact that R/D of any region of the lung is a process that depends on time as well as on the pressure applied to that region. This means that even though the applied pressure to a particular derecruited region might exceed its critical opening pressure, there is a time lag before it is recruited. Similarly, when the applied pressure is released during exhalation, there is a time lag before the region closes.[6] Furthermore, as the lung becomes increasingly injured, longer durations

[*]Department of Anesthesia, University of Iowa, Iowa City, IA 52242, USA

[†]Roy J. Carver Department of Biomedical Engineering, University of Iowa, Iowa City, IA 52242, USA

[‡]Department of Surgery, SUNY Upstate Medical Center, Syracuse, NY 13210, USA

[§]Department of Bioengineering, University of Auckland, Auckland 1124, New Zealand

[‖]Department of Medicine, University of Vermont, Burlington, VT 05405, USA

[¶]Department of Radiology, University of Iowa, Iowa City, IA 52242, USA

Presented as a poster at the 2022 Military Health System Research Symposium, Abstract # MHSRS-22-07335.

doi:https://doi.org/10.1093/milmed/usad059

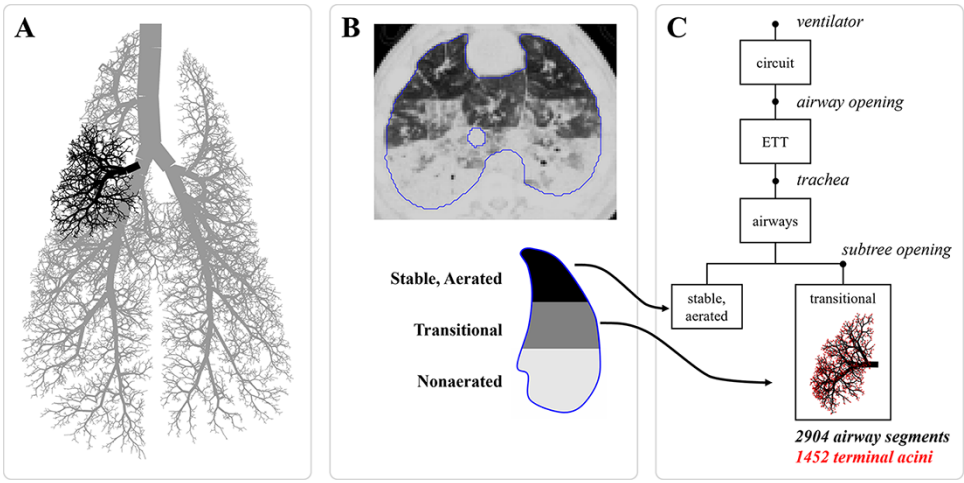

FIGURE 1. (A) Computational model of the porcine lung airway network (gray) generated from a computed tomography scan and the subset of airways (black). (B) Computed tomography image of an injured porcine lung in the transverse section, along with its representation of the three different zones: stable/aerated, transitional, and nonaerated. (C) Complete computational model including a ventilator pressure source, a breathing circuit, an ETT, and the porcine subset of airways consisting of aerated and nonaerated zones, as well as the transitional zone capable of intratidal R/D. Abbreviations: ETT, endotracheal tube.

at high pressure during inspiration are required to produce recruitment, while shorter durations at low pressure during expiration are required for derecruitment to occur.[7] The challenge, therefore, is to adjust the pressure waveforms and durations of inspiration and expiration, such that the necessary minute ventilation can be achieved, while at the same time maximizing the volume of recruited lung and minimizing cyclic R/D.

This is a challenge that is not easily attained, because of the complex and spatially distributed nature of various physiologic factors involved. Nevertheless, airway pressure release ventilation (APRV) has been proposed as a ventilator modality with the attributes required to achieve the aforementioned goals.[7] APRV is a form of positive pressure ventilation that employs a fixed level of high inspiratory pressure (P_{high}) for an extended duration (T_{high}) with brief expiratory durations (T_{low}) at a fixed lower pressure (P_{low}). During APRV, T_{high} may be 80% to 95% of the total breath period, while T_{low} typically ranges from 0.4 to 1.0 s.[8] Studies of APRV in animal models and patients with acute respiratory failure have shown promising clinical and physiological outcomes.[9,10] Nevertheless, our understanding of the beneficial effects of APRV has thus far been limited by the difficulties of studying its mechanistic underpinnings in living subjects.[11] Accordingly, in the present study, we investigated the application of APRV to a porcine model of ARDS using a high-fidelity computational model in which all physiologic mechanisms are specified and thus precisely known. This enabled us to determine how various choices of APRV settings impact regional lung R/D, as well as overall lung mechanics. Portions of this work were presented as a poster at the 2022 Military Health System Research Symposium in Orlando, FL, Abstract number MHSRS-22-07335.

METHODS

The complete computational model used to simulate the APRV waveforms in the injured lung is shown in Figure 1. The computational model was designed to simulate time-varying fluctuations in gas pressure and flow throughout an anatomically structured airway tree with subtending viscoelastic acini. For simplicity, mechanical relationships between gas pressure and flow throughout the model were described using lumped-element representations. Further mathematical details of the simulations can be found in the references cited later. Briefly, the model consisted of a ventilator pressure source, a distensible breathing circuit,[12] an endotracheal tube (ETT),[13] and a porcine lung and chest wall scaled to an approximately 22-kg subject.[14] The inspiratory and expiratory breathing circuit limbs were each assumed to be 1.5 m in length, with a compliance per unit length of 1.2 mL cmH_2O^{-1} m^{-1} and a resistance per unit length of 1 cmH_2O s L^{-1} m^{-1}. The size of the ETT was assumed to be 7.0 mm ID, with a nonlinear pressure-flow relationship as described by Cruz et al.[13] The porcine lung itself was divided into anatomically distinct recruited and derecruited zones, as well as a transitional zone capable of intratidal R/D. The mechanical properties of the consistently recruited zone included a lumped-element representation of the parallel combination of all acini that remained in an opened state during ventilation, in series with a lumped-element representation of the resistive and inertial properties of the airway segments, leading to those recruited acini.[15] The consistently derecruited zone was approximated with an infinite impedance. The transitional zone consisted of a three-dimensional subtree of peripheral airway segments and acini, extracted from a porcine airway tree structure, as previously described.[14] Each airway segment and acinus were modeled using resistive, inertial, and elastic elements,[16]

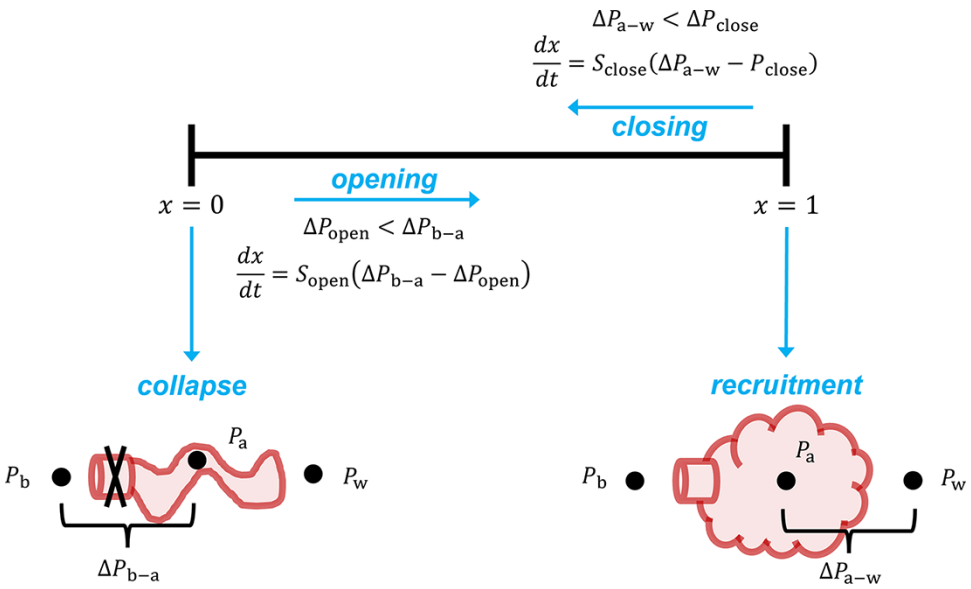

FIGURE 2. Modeling acinar recruitment and derecruitment using a virtual trajectory variable $0 \leq x \leq 1$. During ventilation, x varies according to the distending pressure (ΔP) relative to critical opening (ΔP_{open}) and closing pressures (ΔP_{close}). P_a is the alveolar pressure (inside the lumen). P_b is the pressure at the distal end of the parent bronchiole. P_w is the pressure from the surroundings or stress applied to the wall. ΔP_{b-a} is the driving differential pressure between P_b and P_a. ΔP_{a-w} is the driving differential pressure between P_a and P_w. S_{open} and S_{close} denote rates of opening and closing velocities, respectively. Modified from Bates and Irvin.[6]

with mechanisms to approximate constant-phase viscoelastic tissue impedance,[17] time-dependent acinar R/D,[6] as well as parenchymal strain-stiffening.[18]

Lung injury was simulated by modifying each acinus with an inflation-dependent surface tension randomly sampled from a uniform distribution, to mimic varying degrees of surfactant dysfunction.[19] A numerical solver was implemented to compute gas pressures and flows at each timepoint during the simulation in a manner similar to SPICE solvers,[20] by factoring a large, sparse system of equations constructed *via* modified nodal analysis. Nonlinear elements were substituted by linear approximations for each timestep. An adaptive timestep approach was used to improve numerical stability and reduce computational costs, resulting in simulated time increments ranging from 0.010 to 10.0 msec. Within each iterative timestep, the instantaneous local gas flows and transmural pressures were computed *via* a numerical solver.[20] Regional gas volumes were obtained from numerical integration of the corresponding regional gas flows. The local mechanical properties of the airways and acini, based on the updated local volumes and geometrical assumptions, were then determined, including the R/D state for each acinus.[21]

Recruitment and derecruitment dynamics were represented in the model as pressure- and time-dependent phenomena[6] that mimicked the transient recruitment responses that have been observed experimentally.[22] Each acinus was associated with a virtual trajectory variable x that transitioned gradually from a derecruited state ($x = 0$) to a recruited state ($x = 1$)—or *vice versa*—at a rate proportional to the amount by which the driving pressure exceeded a critical opening or closing pressure threshold (Fig. 2):

$$x(t + \Delta t) = x(t) + \Delta t \frac{dx}{dt} \tag{1}$$

where Δt is the incremental time step and $\frac{dx}{dt}$ is the rate of change in x given by

$$\frac{dx}{dt} = \begin{cases} S_{close}\left(\Delta P_{a-w} - \Delta P_{close}\right), & \text{if } \Delta P_{a-w} < \Delta P_{close} \\ S_{open}\left(\Delta P_{b-a} - \Delta P_{open}\right), & \text{if } \Delta P_{b-a} > \Delta P_{open} \end{cases} \tag{2}$$

S_{open} and S_{close} are speed coefficients for opening and closing, respectively, ΔP_{open} and ΔP_{close} are critical opening and closing pressure thresholds, respectively, ΔP_{b-a} is the difference between the pressure in the parent bronchiole lumen and the pressure in the acinus lumen, and ΔP_{a-w} is the difference between the pressure in the acinus lumen and the stress in the acinar wall. When an acinus was derecruited, its recruitment was driven by the pressure differential between the distal end of its parent airway segment (P_b) and the acinar lumen (P_a), and the critical opening pressure differential was 4 cmH_2O. When the acinus was recruited, its derecruitment was driven by the pressure differential between its lumen (P_a) and the stresses imposed on its septal walls (P_w) (i.e., local transmural pressure). The critical closing pressure differential was 0 cmH_2O. Opening and closing rate variables were randomly sampled from an inverse uniform distribution with a minimum value of 0.1 s^{-1} cmH_2O^{-1}. Acini were immediately derecruited if luminal volume decreased below a limiting threshold representing the residual gas volume of the acinus.

The original anatomic structure of the porcine model consisted of 30,959 cylindrical airway segments, with 15,479

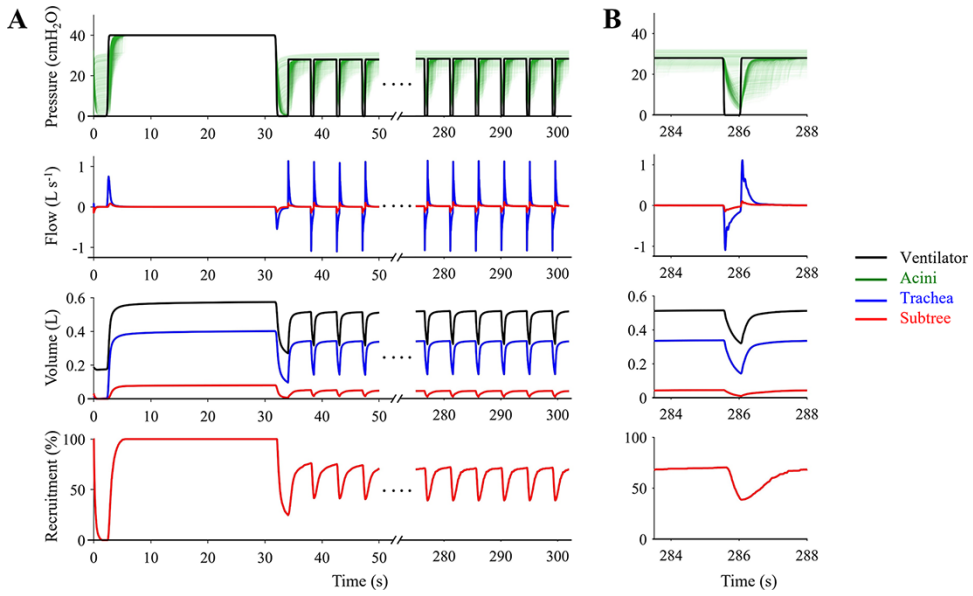

FIGURE 3. (A) Example of the porcine computational lung model under a recruitment maneuver to 40 cmH_2O, followed by APRV with $P_{high} = 28\ cmH_2O$, $T_{high} = 4.0$ sec, $T_{low} = 0.5$ sec, and transitional to aerated lung volumes = 0.20. The figure shows the first 50 seconds and the last APRV breaths of the simulation. The individual acinar pressures within the subtree are shown in green, while black denotes the ventilator pressure waveform proximal to the breathing circuit. Flow at the trachea and subtree are shown in blue and red, respectively. Total volume from the ventilator, volume at the trachea, and volume at the subtree are shown in black, blue, and red, respectively. Acinar recruitment reached 100% during the recruitment maneuver but remains irregular during the APRV with $T_{low} = 0.5$ sec. (B) Close up of the same waveforms as in (A), from times 284 to 288 seconds of the simulation. Abbreviations: APRV, airway pressure release ventilation.

viscoelastic acini.[14] This geometry allowed for different, albeit limited, options for selecting a specific subsegmental branch of the airway tree, as well as the size of its subtree. Simulations required approximately 150 h of computing time for 300 seconds of simulation time, using 14 threads of a high-performance computing cluster. Given such a high computational overhead, we selected a transitional subtree with roughly 10% (1,452 acini) of the total number of viscoelastic acini in the original model. Model simulations were performed with three different scenarios of varying percentages of aerated, nonaerated, and transitional compartments comprising the total lung volume: scenario I—45% consistently aerated, 9% transitional, and 46% consistently nonaerated; scenario II—60% consistently aerated, 9% transitional, and 31% consistently nonaerated; and scenario III—90% consistently aerated, 9% transitional, and 1% consistently nonaerated. Thus, the corresponding ratios of transitional to aerated (T/A) lung volumes for scenarios I, II, and III were 0.20, 0.15, and 0.10, respectively, progressing through decreasing severities of lung injury.

The ventilator pressure source of the model simulated APRV waveforms with P_{high} of 28 and 40 cmH_2O, T_{high} of 4.0 seconds, P_{low} of 0 cmH_2O, and T_{low} ranging from 0.2 to 1.5 seconds in 0.1 second increments. These values of P_{high}, T_{high}, P_{low}, and T_{low} were selected to explore the roles of parenchymal strain stiffening and R/D in our simulations, as reported in our recent experimental study in pigs.[5] Each simulation was initiated with a 30 second recruitment maneuver to 40 cmH_2O followed by 60 breaths, each of total duration $T_{high} + T_{low}$. The last five breaths were used to calculate the percentages of sustained recruitment, as well as intratidal R/D, in the transitional zone. The estimated "global" elastances of the transitional subtree, as well as the entire porcine respiratory system comprising the consistently recruited, transitional, and consistently derecruited compartments of the lung, were obtained using the multiple linear regression technique described by Kaczka et al.[23] Global resistive and elastic properties for the subtree and the entire respiratory system were estimated from the corresponding sampled flow and pressure waveforms at the subtree root and the trachea, respectively, using the equation of motion,

$$P = R\dot{V} + EV + P_0 \quad (3)$$

where P, $\dot{V}$, and V denote the delivered pressure, flow, and volume, respectively, at the trachea or subtree root, R is the resistance, E is the elastance, and P_0 is the distending pressure at end expiration. Estimates of the R, E, and P_0 parameters for the total respiratory system and subtree were obtained from the last five APRV breaths for each simulation.

RESULTS

Figure 3 shows example pressure, flow, and volume tracings simulated by the computational model over 50 seconds, as well as the percentage of acinar recruitment in the transitional subtree. For this simulation, the ratio of the relative percentages of transitional and aerated volume (T/A) was equal to 0.20. The simulation started with all acini of

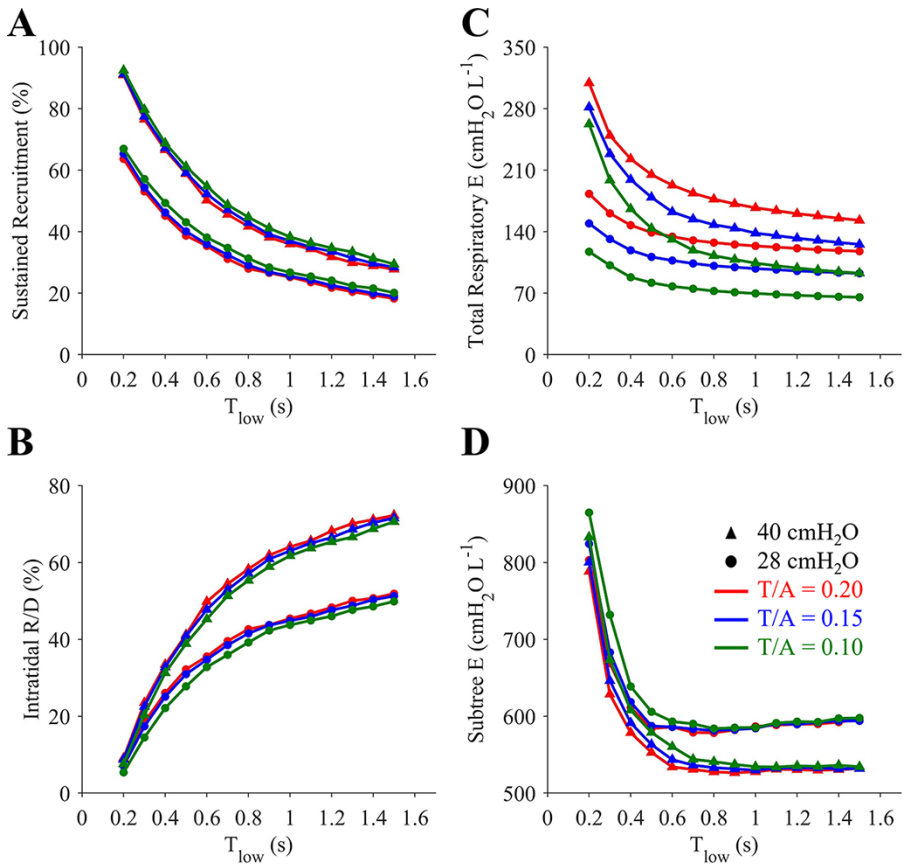

FIGURE 4. (A) Sustained acinar recruitment, (B) intratidal R/D, (C) total respiratory E, and (D) subtree E vs. T_{low}. Simulations were obtained for P_{high} of 28 (circles) and 40 (triangles) cmH_2O for the three different ratios of transitional and aerated zones (T/A). Abbreviations: R/D, cyclic recruitment and derecruitment.

the subtree derecruited, followed by a recruitment maneuver to 40 cmH_2O and then cyclic APRV breaths with $P_{high} = 28\ cmH_2O$, $P_{low} = 0\ cmH_2O$, $T_{high} = 4.0$ seconds, and $T_{low} = 0.5$ seconds. Note that 100% of the acini in the subtree were recruited within 2.27 seconds of the ventilator pressure reaching 40 cmH_2O. However, during the APRV breaths, acinar recruitment in the transitional subtree was ongoing during T_{high}, varying between a minimum of 40% at end expiration and a peak value of about 75% at end inspiration.

Figure 4A shows the sustained acinar recruitment vs. T_{low} within the subtree, defined as the percentage of those acini in the subtree remaining in a consistently opened state during APRV (i.e., the percent recruitment within the transitional subtree at end expiration). Simulations are shown for $P_{high} = 40\ cmH_2O$ and 28 cmH_2O and T/A ratios of 0.20, 0.15, and 0.10. Sustained acinar recruitment in the subtree was consistently higher for $P_{high} = 40\ cmH_2O$ compared with 28 cmH_2O, regardless of T_{low} or T/A ratio. However, for both P_{high} values, sustained recruitment in the subtree decreased with increasing T_{low}. There was essentially no influence of the T/A ratio on sustained recruitment, regardless of P_{high}. Figure 4B shows the corresponding percentages of acini within the subtree experiencing intratidal R/D, defined as the relative number of acini cycling between opened and closed states during the APRV breaths. The percentage of intratidal R/D was higher for $P_{high} = 40\ cmH_2O$ compared with 28 cmH_2O and increased with increasing T_{low}, from 7% to 51% for $P_{high} = 28\ cmH_2O$, and from 8% to 71% for $P_{high} = 40\ cmH_2O$. Intratidal R/D was only minimally affected by T/A ratio.

Figure 4C shows the estimated E of the total respiratory system vs. T_{low} for $P_{high} = 28$ and 40 cmH_2O, as well as the three different percentages of aerated, nonaerated, and transitional zones. For all conditions, respiratory E decreased with increasing T_{low}, with a steeper descent for $P_{high} = 40\ cmH_2O$ compared with 28 cmH_2O. Moreover, respiratory E increased with the increasing T/A ratio, regardless of P_{high}. For each T/A ratio, respiratory E was higher for $P_{high} = 40\ cmH_2O$ compared with 28 cmH_2O, regardless of T_{low}.

Figure 4D shows the estimated E of the transitional subtree vs. T_{low} for $P_{high} = 28$ and 40 cmH_2O, as well as the three different percentages of aerated, nonaerated, and transitional zones. Similar to the estimations for the total respiratory system model, the subtree E decreased with increasing T_{low} for expiratory durations less than about 0.7 seconds. For both P_{high} conditions of 40 and 28 cmH_2O, the subtree E

achieved a plateau in T_{low} greater than 0.7 seconds. Above this level of T_{low}, the subtree E diverged for the two P_{high} levels, being higher for 28 cmH_2O compared with 40 cmH_2O. However, at each P_{high} level, the subtree elastance exhibited no dependence on the T/A ratio.

DISCUSSION

Supportive mechanical ventilation remains the mainstay of clinical management for many forms of acute lung injury and respiratory failure, especially in patients who meet the clinical criteria for ARDS. Regardless of etiology, ARDS remains a major contributor to mortality in critically ill patients.[24] However, if ventilator settings are not appropriate for a given patient, unintended VILI may arise, further contributing to the mortality associated with ARDS.[25]

The pathophysiology of ARDS is often conceptualized with the aid of compartmentalized representations of the lung, as shown in Figure 1B. One compartment represents consistently aerated (i.e., recruited) lung tissue, and another compartment represents non-recruitable and/or edematous tissue, while a third compartment represents a "transitional" zone consisting of tissue that can experience intratidal R/D. Among various mechanisms postulated to cause VILI in ARDS, the two principle candidates are (1) overdistension of alveoli in the consistently aerated compartment (i.e., volutrauma) and (2) cyclic R/D of alveoli in the transitional compartment (i.e., atelectrauma).[21] "Protective" ventilation strategies in ARDS are designed to minimize volutrauma in the consistently aerated compartment using reduced tidal volumes or driving pressures while simultaneously providing appropriate levels of positive end-expiratory pressure to maintain lung recruitment in the transitional compartment. This allows the collapsed tissue to "rest" by keeping it out of the ventilator cycle. However, such protective strategies have not dramatically lowered mortality in patients with established ARDS[24,26,27] despite their widespread adoption and persistent use in clinical practice. One reason for this disappointing outcome may be the longitudinal time course of the mechanical derangements in ARDS. That is, as more aerated tissue is progressively lost to gradual alveolar collapse, more injurious strain is placed on the parenchyma of the remaining aerated lung.[28] Accordingly, if a progressively shrinking functional lung is at the core of VILI pathophysiology, then countermeasures that avoid such shrinkage may improve clinical outcomes.[7]

APRV was first introduced in 1987[29] as a supportive ventilator modality that essentially provides continuous positive airway pressure to the airway opening for maintenance of lung recruitment interspersed with brief periodic interruptions to guarantee a minimal level of CO_2 elimination. In contrast to conventional ventilator modalities that are restricted to ventilating a heterogeneously injured lung and so rely on low tidal volumes or driving pressures to minimize the potential for parenchymal overdistention, APRV uses extended inspirations to progressively recruit lung tissue over prolonged periods of time. Most importantly, APRV employs expiratory durations that are short enough such that the recruited lung does not have enough time to derecruit before inspiration begins again. In this way, APRV has potential to recruit alveoli and prevent their recollapse with each breath, thus preventing progressive collapse. This inflate (rapid inspiration from the termination of expiration) and brake (brief expiratory duration preventing alveolar recollapse) effectively "ratchets" open small volumes of lung with each breath slowly recruiting the entire lung over a period of hours,[7] similar to the method the full-term newborn uses to "ratchet" open their collapsed and fluid filled lungs at birth.[30] However, the appropriate APRV settings to apply to a given patient remain a matter of contention.[31]

In this study, we used a computational model to simulate how the APRV parameters P_{high} and T_{low} influence the dynamic acinar recruitment patterns in the transitional zone of the lung. The model is based on realistic airway anatomy, accounts for both the pressure and time dependencies of R/D, and produces ventilator waveforms strongly reminiscent of those observed clinically (Fig. 3). The model also simulates the dynamic state of lung recruitment, which enabled us to show that for a given P_{high}, decreasing T_{low} increased the sustained recruitment of unstable acini and thus reduced intratidal R/D (Fig. 4A and B). These recruitment patterns were independent of the relative amounts of consistently recruited and derecruited lung tissue (i.e., the T/A ratio). Increasing P_{high} also increased the sustained recruitment of unstable acini (Fig. 4A), but at the expense of an increase in intratidal R/D, especially as T_{low} increased (Fig. 4B). Since intratidal R/D is recognized as a key contributor to atelectrauma and VILI, our simulations thus suggest that the most critical APRV parameter is T_{low}. Regardless of the value of P_{high}, T_{low} should be kept as low as physiologically permissible, permitting only just enough exhaled volume to maintain adequate CO_2 elimination and no more. Nonetheless, T_{low} should remain sufficiently brief to prevent atelectrauma induced by large increases in intratidal R/D.

As expected, estimates of total respiratory system E at a given P_{high} increased with the increasing T/A ratio (Fig. 4C), consistent with reductions in aerated volume and the amount of functional lung tissue in communication with the airway opening (i.e., the "baby lung"). Moreover, for a given T/A ratio, increasing P_{high} from 28 to 40 cmH_2O resulted in increased E at all values of T_{low}, consistent with the strain stiffening of the parenchymal tissues that was incorporated into our model.[18] Similarly, the apparent elastances of both the total porcine respiratory system and the subtree decreased with increasing T_{low} regardless of P_{high} or T/A ratio (Fig. 4C and D), consistent with a greater fraction of the recruited acini being on a flatter portion of their pressure–volume curves throughout the breathing cycle.[18] Thus, the improvements in sustained lung recruitment with decreasing T_{low} resulted in higher acinar distending pressures and thus higher E. On the other hand, higher P_{high} also resulted

in increased R/D (Fig. 4B) because higher inspiratory pressures recruit more severely injured acini that tend to have faster rates of collapse. Our model simulations thus suggest that higher inspiratory pressures should be used in conjunction with shorter exhalation times to avoid increasing the damaging effects of intratidal R/D.

The computational modeling and simulation study presented here offer several insights into the mechanical properties and dynamics of recruitment of the acutely injured lung during APRV. Nonetheless, our study does have a number of limitations. First, a porcine structure was used for our simulations,[14] given our previously acquired data on regional mechanics using computed tomography imaging in pig lungs.[11,32,33] Moreover, the pig lung is sufficiently large in size, such that its mechanical properties are similar enough to those of human lungs for these results to be relevant for clinical applications. In addition, we used an empiric model of R/D dynamics[6] and thus did not distinguish between cyclic acinar collapse and axial movement of liquid plugs along small airways, which may also be an important contributor to apparent intratidal recruitment. The effects of parenchymal interdependence among the acini in our subtree were also not accounted for in these simulations.[34] Such mechanical interdependence may strongly influence R/D dynamics and result in the clustering of "stress concentrators," further contributing to VILI.[2] Other factors of course may also contribute to VILI, such as barotrauma as well as heart/lung interactions. Moreover, as an investigation solely on the influence of APRV on respiratory mechanics and recruitment patterns, our study did not consider the effects of APRV on hemodynamics, gas exchange, or ventilation-to-perfusion matching. Finally, while we did consider different severities of lung injury based on the level of sustained derecruitment, we did not account for time-varying changes in the mechanical properties of the model over long durations, as may be seen over the course of hours or days in patients with ARDS.[7] Such time-varying changes could potentially be incorporated into the mechanical properties of the model, which would allow for real-time adjustments in the APRV settings. While such "long-duration" simulations of mechanical ventilation are computationally prohibitive at the present time, they will certainly become feasible in the future as processing speed improves.

In conclusion, these simulations using an anatomically based computational model of the ventilated injured lung demonstrate the confounding effects of cyclic R/D, sustained recruitment, and parenchymal strain stiffening on estimates of global and regional elastance during APRV. Minimally injurious ventilation strategies thus cannot be based simply on minimizing lung elastance; one must consider competing physiologic phenomena when choosing ventilator settings for a given patient. Moreover, a major difference between the current protective ventilation strategies and APRV is that the former is constrained to ventilating a heterogeneously injured lung, whereas the latter recruits the entire lung over a period of hours, allowing the possibility of repair during its naturally inflated state. Determination of the least injurious APRV settings, however, is a significant challenge given the complexities of the various factors involved. Our model has the potential to play a valuable role in guiding such decisions, particularly when combined with patient-specific evidence of R/D and parenchymal strain stiffening.[11,33]

SUPPLEMENT SPONSORSHIP

This article appears as part of the supplement "Proceedings of the 2022 Military Health System Research Symposium," sponsored by the Assistant Secretary of Defense for Health Affairs.

ACKNOWLEDGMENTS

This research was supported in part through computational resources provided by The University of Iowa, Iowa City, Iowa

FUNDING

Supported in part by the Department of Defense, Office of the Assistant Secretary of Defense for Health Affairs, through the Peer-Reviewed Medical Research Program under Award Numbers W81XWH-20-1-0696 and W81XWH-21-1-0507.

CONFLICT OF INTEREST STATEMENT

Opinions, interpretations, conclusions, and recommendations are those of the authors and are not necessarily endorsed by the Department of Defense. M.K.-S. has received a Research Grant, and G.F.N. an Unrestricted Educational Grant from Dräger Medical Systems, Inc. G.F.N. and M.K.-S. have presented and received honoraria and/or travel reimbursement at event(s) sponsored by Dräger Medical Systems, Inc., outside of the published work. G.F.N. and M.K.-S. have lectured for Intensive Care Online Network, Inc. (ICON). D.W.K. and J.H. are a co-founders, officers, and shareholders of OscillaVent, Inc., as well as co-inventors on a patent involving multifrequency oscillatory ventilation. D.W.K. and J.H. also received research support from ZOLL Medical Corporation. D.W.K. has a consulting agreement with Lungpacer Medical, Inc. J.H.T.B. is a consultant to and shareholder of OscillaVent, Inc. and has two patents pending in the field of mechanical ventilation. The authors attest that industry had no role in the design and conduct of this study, the collection, management, analysis, or interpretation of the data, nor the preparation, review, or approval of the manuscript.

REFERENCES

1. Morris MJ: Acute respiratory distress syndrome in combat casualties: military medicine and advances in mechanical ventilation. Mil Med 2006; 171(11): 1039–44. 10.7205/MILMED.171.11.1039.
2. Gaver DP 3rd, Nieman GF, Gatto LA, Cereda M, Habashi NM, Bates JHT: The POOR get POORer: a hypothesis for the pathogenesis of ventilator-induced lung injury. Am J Respir Crit Care Med 2020; 202(8): 1081–7. 10.1164/rccm.202002-0453CP.
3. Cereda M, Xin Y, Goffi A, et al: Imaging the injured lung: mechanisms of action and clinical use. Anesthesiology 2019; 131(3): 716–49. 10.1097/ALN.0000000000002583.
4. Cereda M, Xin Y, Hamedani H, et al: Tidal changes on CT and progression of ARDS. Thorax 2017; 72(11): 981–9. 10.1136/thoraxjnl-2016-209833.
5. Ramcharran H, Bates JHT, Satalin J, et al: Protective ventilation in a pig model of acute lung injury: timing is as important as pressure. J Appl Physiol (1985) 2022; 133(5): 1093–105. 10.1152/japplphysiol.00312.2022.
6. Bates JHT, Irvin CG: Time dependence of recruitment and derecruitment in the lung: a theoretical model. J Appl Physiol (1985) 2002; 93(2): 705–13. 10.1152/japplphysiol.01274.2001.

7. Nieman G, Kollisch-Singule M, Ramcharran H, et al: Unshrinking the baby lung to calm the VILI vortex. Crit Care 2022; 26(1): 242. 10.1186/s13054-022-04105-x.
8. Fredericks AS, Bunker MP, Gliga LA, et al: Airway pressure release ventilation: a review of the evidence, theoretical benefits, and alternative titration strategies. Clin Med Insights Circ Respir Pulm Med 2020; 14: 1179548420903297. 10.1177/1179548420903297.
9. Andrews PL, Shiber JR, Jaruga-Killeen E, et al: Early application of airway pressure release ventilation may reduce mortality in high-risk trauma patients: a systematic review of observational trauma ARDS literature. J Trauma Acute Care Surg 2013; 75(4): 635–41. 10.1097/TA.0b013e31829d3504.
10. Carsetti A, Damiani E, Domizi R, et al: Airway pressure release ventilation during acute hypoxemic respiratory failure: a systematic review and meta-analysis of randomized controlled trials. Ann Intensive Care 2019; 9(1): 44. 10.1186/s13613-019-0518-7.
11. Herrmann J, Gerard SE, Shao W, et al: Effects of lung injury on regional aeration and expiratory time constants: insights from four-dimensional computed tomography image registration. Front Physiol 2021; 12: 707119. 10.3389/fphys.2021.707119.
12. Herrmann J, Fonseca da Cruz A, Hawley ML, Branson RD, Kaczka DW: Shared ventilation in the era of COVID-19: a theoretical consideration of the dangers and potential solutions. Respir Care 2020; 65(7): 932–45. 10.4187/respcare.07919.
13. Cruz AF, Herrmann J, Carvalho CRR, Kaczka DW: A comparison of endotracheal tube compensation techniques for the measurement of respiratory mechanical impedance at low frequencies. J Clin Monit Comput 2022; 36(5): 1461–77. 10.1007/s10877-021-00788-9.
14. Herrmann J, Tawhai MH, Kaczka DW: Strain, strain rate, and mechanical power: an optimization comparison for oscillatory ventilation. Int J Numer Method Biomed Eng 2019; 35(10): e3238. 10.1002/cnm.3238.
15. Kennelly AE: Equivalence of triangles and stars in conducting networks. Electr World Eng 1899; 34(12): 413–314.
16. Colletti AA, Amini R, Kaczka DW: Simulating ventilation distribution in heterogeneous lung injury using a binary tree data structure. Comput Biol Med 2011; 41(10): 936–45. 10.1016/j.compbiomed.2011.08.004.
17. Kaczka DW, Smallwood JL: Constant-phase descriptions of canine lung, chest wall, and total respiratory system viscoelasticity: effects of distending pressure. Respir Physiol Neurobiol 2012; 183(2): 75–84. 10.1016/j.resp.2012.06.008.
18. Salazar E, Knowles JH: An analysis of pressure-volume characteristics of the lungs. J Appl Physiol (1985) 1964; 19(1): 97–104. 10.1152/jappl.1964.19.1.97.
19. Herrmann J, Lilitwat W, Tawhai MH, Kaczka DW: High-frequency oscillatory ventilation and ventilator-induced lung injury: size does matter. Crit Care Med 2020; 48(1): e66–73. 10.1097/CCM.0000000000004073.
20. Nagel NW: *SPICE2: A Computer Program to Simulate Semiconductor Circuits*. University of California; 1975.
21. Amini R, Herrmann J, Kaczka DW: Intratidal overdistention and derecruitment in the injured lung: a simulation study. IEEE Trans Biomed Eng 2017; 64(3): 681–9. 10.1109/TBME.2016.2572678.
22. Massa CB, Allen GB, Bates JHT: Modeling the dynamics of recruitment and derecruitment in mice with acute lung injury. J Appl Physiol (1985) 2008; 105(6): 1813–21. 10.1152/japplphysiol.90806.2008.
23. Kaczka DW, Barnas GM, Suki B, Lutchen KR: Assessment of time-domain analyses for estimation of low-frequency respiratory mechanical properties and impedance spectra. Ann Biomed Eng 1995; 23(2): 135–51. 10.1007/BF02368321.
24. Rezoagli E, Fumagalli R, Bellani G: Definition and epidemiology of acute respiratory distress syndrome. Ann Transl Med 2017; 5(14): 282. 10.21037/atm.2017.06.62.
25. Slutsky AS, Ranieri VM: Ventilator-induced lung injury. N Engl J Med 2013; 369(22): 2126–36. 10.1056/NEJMra1208707.
26. Bellani G, Laffey JG, Pham T, et al: Epidemiology, patterns of care, and mortality for patients with acute respiratory distress syndrome in intensive care units in 50 countries. JAMA 2016; 315(8): 788–800. 10.1001/jama.2016.0291.
27. Phua J, Badia JR, Adhikari NK, et al: Has mortality from acute respiratory distress syndrome decreased over time?: a systematic review. Am J Respir Crit Care Med 2009; 179(3): 220–7. 10.1164/rccm.200805-722OC.
28. Marini JJ, Gattinoni L: Time course of evolving ventilator-induced lung injury: the "Shrinking Baby Lung". Crit Care Med 2020; 48(8): 1203–9. 10.1097/CCM.0000000000004416.
29. Downs JB, Stock MC: Airway pressure release ventilation: a new concept in ventilatory support. Crit Care Med 1987; 15(5): 459–61. 10.1097/00003246-198705000-00001.
30. Tingay DG, Farrell O, Thomson J, et al: Imaging the respiratory transition at birth: unraveling the complexities of the first breaths of life. Am J Respir Crit Care Med 2021; 204(1): 82–91. 10.1164/rccm.202007-2997OC.
31. Jain SV, Kollisch-Singule M, Sadowitz B, et al: The 30-year evolution of airway pressure release ventilation (APRV). Intensive Care Med Exp 2016; 4(1): 11. 10.1186/s40635-016-0085-2.
32. Herrmann J, Gerard SE, Reinhardt JM, Hoffman EA, Kaczka DW: Regional gas transport during conventional and oscillatory ventilation assessed by xenon-enhanced computed tomography. *Ann Biomed Eng* 2021; 49(9): 2377–88. 10.1007/s10439-021-02767-2.
33. Herrmann J, Gerard SE, Shao W, et al: Quantifying regional lung deformation using four-dimensional computed tomography: a comparison of conventional and oscillatory ventilation. Front Physiol 2020; 11: 14. 10.3389/fphys.2020.00014.
34. Roth CJ, Ismail M, Yoshihara L, Wall WA: A comprehensive computational human lung model incorporating inter-acinar dependencies: application to spontaneous breathing and mechanical ventilation. Int J Numer Method Biomed Eng 2017; 33(1). 10.1002/cnm.2787.